

Portable X-ray fluorescence and clustering methods applied to mineral exploration: the significance and nature of Batigelas anomaly (Ossa-Morena Zone - Cabeço de Vide, Portugal)

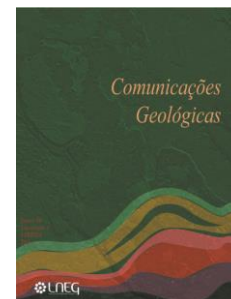
Fluorescência de raios-X portátil e métodos de clustering aplicados à prospeção mineral: significado e natureza da anomalia de Batigelas (Zona de Ossa-Morena - Cabeço de Vide, Portugal)

P. Nogueira^{1,2*}, P. Afonso^{1,3}, J. Roseiro^{1,2}, M. Maia^{1,2}, D. São Pedro^{1,2}, N. Moreira^{1,2}, J. X. Matos⁴, M. J. Batista⁵

Recebido em 05/12/2019 / Aceite em 24/01/2020

Publicado online em julho de 2020

© 2020 LNEG – Laboratório Nacional de Energia e Geologia IP



Artigo original
Original article

Abstract: Batigelas is a mineral occurrence in the Alter do Chão-Elvas Sector of the Ossa-Morena Zone that was studied by the Serviço de Fomento Mineiro, including soil geochemistry and terrestrial geophysics, revealing anomalous metal contents combined with contrasting magnetic values. The results obtained justified the execution of a cored drill hole. New soil geochemistry campaign, using a portable X-ray fluorescence, has yielded new detailed results, with a set of elemental analysis for the region. The application of clustering methods (hierarchical and k-means clustering) to the analyses allowed to detail not only the initial anomaly identified, but also to discriminate the outcropping lithological units in the region. The obtained results highlight the presence of a cryptic Zn-Pb anomalous occurrence, thus emphasizing the importance of these techniques in mineral exploration campaigns, providing new exploration pathfinders.

Keywords: Batigelas, portable X-ray fluorescence, k-means clustering, hierarchical clustering.

Resumo: Batigelas é uma ocorrência mineral no Setor de Alter do Chão-Elvas, Zona de Ossa-Morena, que foi estudada pelo Serviço de Fomento Mineiro através da avaliação geoquímica de solos e geofísica terrestre, métodos que revelaram conteúdos anómalos em metais base, bem como um contraste acentuado das propriedades magnéticas na região. Os resultados obtidos justificaram a realização de uma sondagem carotada. Trabalhos recentes de geoquímica de solos, com recurso a uma fluorescência de raios-X portátil, permitiram obter resultados detalhados de análises elementares fundamentais para a caracterização geoquímica da região. A aplicação de métodos de clustering (aglomeração hierárquica e k-média) para a análise dos dados permitiram, não só pormenorizar a anomalia identificada inicialmente como também identificar as unidades litológicas aflorantes na região. Os resultados obtidos permitiram identificar uma nova ocorrência anómala de Zn-Pb, salientando a importância da aplicação desta técnica em situações de prospeção mineral, com a identificação de guias geoquímicos.

Palavras-chave: Batigelas, fluorescência de raios-X portátil, aglomeração k-média, aglomeração hierárquica.

1. Introduction

Throughout the 50s until the 70s decades of the 20th century, the Serviço de Fomento Mineiro (SFM), as a governmental organization, conducted a systematic campaign of geological, geochemical and geophysical recognition as a support for mineral exploration, namely in the Ossa-Morena Zone (OMZ). The different activities included rock and soil sampling, the later usually in a regular grid, combined with geophysical measurements, where magnetic and gravimetric approaches were the most common and, when justified, some cored drill holes were performed. This sampling was later used for geochemical analysis of the rocks and soils collected. One of the expeditious techniques used for geochemical characterization of soils was a colorimetric test that identifies and relatively quantifies the presence of heavy metals in soils, where copper, lead and zinc are the most usual elements. The results provided a bulk value for heavy metals, in ppm, not distinguishing between the several elements present. Seldom, when in the presence of a heavy metal anomaly, that could be combined with geophysical favourable indicators, the execution of a cored drill hole to evaluate the metalliferous potential was justified.

Batigelas, located in the Alter do Chão-Elvas Sector (ACES), is an example of an anomalous occurrence of heavy metals in soils, with obvious contrast to the regional geochemical background. A contrasting geophysical magnetic anomaly was also identified near the Batigelas geochemical anomaly. A cored drill hole was carried out, northeast of the geochemical anomaly inclined 45° towards N217°, with the intention of crosscutting the main geological features, as the structure in this sector dips towards northeast. The core log indicates several lithotypes - from top to bottom - conglomerates, calc-silicate rocks and mafic intrusive rocks, the last two with sulphide (e.g. pyrrhotite, chalcopyrite and pyrite) and oxide phases (Afonso, in Prep.); however, the mafic rocks with sulphides do not seem to be related with the Batigelas anomaly. Notwithstanding the promising results, no further studies in Batigelas anomaly were conducted, after these first outcomes.

Some exploration companies were interested in the regional abundance of base metals and platinoids (e.g. Pinto *et al.*, 2006),

¹ Departamento de Geociências da Escola de Ciências e Tecnologia da Universidade de Évora. Apartado 94, 7000 Évora, Portugal.

² Instituto de Ciências da Terra, Apartado 94, 7000 Évora, Portugal.

³ Departamento de Física da Escola de Ciências e Tecnologia da Universidade de Évora. Apartado 94, 7000 Évora, Portugal.

⁴ Laboratório Nacional de Energia e Geologia (LNEG), Campus de Aljustrel; Bairro da Vale d'oca 14, 7601-909 Aljustrel, Portugal.

⁵ Laboratório Nacional de Energia e Geologia (LNEG), Apartado 7586, Alfragide, 2610-999 Amadora, Portugal

*Autor correspondente/Corresponding author: pmn@uevora.pt

but the published reports demonstrate that Batigelas was not an area that was further investigated in these campaigns.

During last year, the ZOM-3D project (see acknowledgments) selected Batigelas as one of the selected mineral occurrences to conduct additional studies. This work presents the results of geochemical analysis *in situ* using a portable X-ray fluorescence equipment. The application of unsupervised machine learning techniques to the geochemical data, namely clustering methods, was performed in order to provide a better understanding of the recognized anomalies.

2. Geological background

The ACES of the OMZ (SW Iberian Variscides) comprises a Neoproterozoic to Middle Cambrian volcano-sedimentary succession (Oliveira *et al.*, 1991; Araújo *et al.*, 2013; Moreira *et al.*, 2014a), showing a NW-SE regional trend related with the Variscan main tectono-metamorphic episodes (Araújo *et al.*, 2013; Moreira *et al.*, 2014b). This metasedimentary succession is intruded by distinct magmatic rocks (Gonçalves, 1972; Carrilho Lopes 1989; Carrilho Lopes *et al.*, 1993; Sant’Ovaia *et al.*, 2013), defining the main lithological units of this sector. Specifically, in this sector crops out an intrusive mafic-ultramafic complex (Alter do Chão – Cabeço de Vide Complex) and some peralkaline rocks (NE Alentejo peralkaline transect) of Cambrian-Ordovician ages (Lancelot and Allégret, 1982; Carrilho Lopes *et al.*, 1993; Díez Fernández *et al.*, 2014), affected by regional metamorphism. Additionally, a late Carboniferous granitoid complex (Santa Eulalia Plutonic Complex; Serrano Pinto, 1984; Carrilho Lopes *et al.*, 2013; Pereira *et al.*, 2017) crosscuts all the previous mentioned lithological units.

The Batigelas mineral occurrence (Fig. 1) is located in the northern part of the ACES, near the Alter do Chão Thrust, which outline the contact with the Blastomylonitic Belt (BMB; Gonçalves, 1972; Oliveira *et al.*, 1991; Araújo *et al.*, 2013), here composed of high grade rocks of the Série Negra Succession, comprising micaschists and black metacherts/metalydites with Late Ediacaran ages (*e.g.* Gonçalves, 1972; Oliveira *et al.*, 1991; de Oliveira *et al.*, 2003; Pereira *et al.*, 2006). Southwest from Batigelas the Alter do Chão – Cabeço de Vide Mafic-Ultramafic complex crops out and, surrounding this intrusion, an aureole of contact metamorphism with calc-silicate hornfels rocks is identified (Gonçalves, 1972), showing the temporal relationship between this plutonic complex and the Neoproterozoic-Cambrian succession.

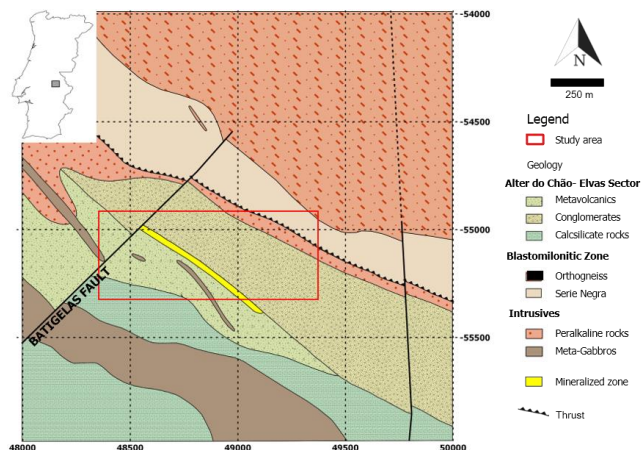


Figure 1. Geological setting of the Batigelas area. Adapted from Sheet 32-B Portalegre, 1:50 000 (Gonçalves, 1972).

Figura 1. Enquadramento geológico da área de Batigelas. Adaptado da Folha 32-B Portalegre, 1/50 000 (Gonçalves, 1972).

3. Methods

Herein the results of a high-resolution geochemical soil campaign (50m×50m) are presented and discussed. The soil analyses were performed *in situ*, using a portable X-Ray Fluorescence (pXRF) from Skyray Instruments, in a regular mesh (20×8=160 points) around the historic drill hole, site where the most interesting results (‘Mineralized Zone’; Fig. 1) were identified by the SFM. The ‘Mineral Mode’ of the equipment (commonly named ‘Mining Mode’; Hall *et al.*, 2013) was used. All the analysis were performed in a homogenised and hand milled soil spot (defined as ‘mole heap’; Lemiere, 2018), using the predefined settings for this type of analysis, with a duration of 60 seconds for each run. The pXRF equipment detected nine major elements including SiO₂, Al₂O₃, MgO, Fe₂O₃, CaO, K₂O, MnO, TiO₂ and P₂O₅, and fifteen trace elements: Sr, Rb, Zr, V, Cr, Ni, Sn, Cu, Zn, Pb, As, Mo, Ga, Nb and Y.

The MgO, Al₂O₃, Ga and Mo were not used in this study (light grey and bold in table 1) as they were detected in a reduced number of samples (<50% of total samples) and, therefore, lack statistical significance. It must be emphasized that pXRF analyses have some limitations as previous described (Hou *et al.*, 2004; Hall *et al.*, 2013; Bourke and Ross, 2014; Lemiere, 2018), the same constraints apply to our study, namely the detection limits and the possible interferences between elements. Independently from these constraints, the results are in accordance with the lithological, geochemical and structural data which characterize the units previously described in SFM works.

Statistical analysis was conducted on the elemental data, and the correspondent descriptive results are shown in table 1. A multivariate statistical approach, through the computation of hierarchical and k-means clustering, was performed using the R programming language (R Core Team, 2014). The interpolated maps were generated using the Inverse Distance Weighted method (Isaaks and Srivastava, 1989) with a factor of 2 and a pixel size of 10 meters.

4. Geochemical data and their significance

4.1. Exploratory data analysis

The SFM campaign covered a 4 km×2 km area, with a sampling grid of 100m×100m. Figure 2 shows the interpolated results for the heavy metals spatial distribution within the surveyed area. This geochemical map clearly identifies a heavy metals anomalous zone that aligns with the regional NW-SE trend perfectly overlapping the SFM mineralized zone (Fig. 1). The high-resolution pXRF campaign was conducted in this zone with the intention of detailing their results, with a denser grid for the identified and quantified elements.

For some of the major elements (CaO, MnO, Fe₂O₃) the interpolated maps show a gradient of values that can be related with the lithological units, separating two distinct areas (Fig. 3): (1) the southwest area, with high CaO, MnO and Fe₂O₃ contents, mainly composed of calc-silicate and metavolcanics, and (2) the northeast area, with conglomerates and peralkaline rocks, depleted in these elements. The patterns show a NW-SE general trend, in accordance with the direction of geological structures and lithological units of SFM (Fig. 1). For some of the trace elements (*i.e.* V, Zr, Cr, Cu and Ni) the same chemical distribution is also emphasized (see V, Cr and Cu examples in figure 3). The interpolated maps for another group of elements, specifically As, Pb and Zn (Fig. 3), reveal a different pattern matching with the presence of the mineralized zone, similarly NW-SE general direction. Besides these recognizable patterns,

Table 1. Descriptive statistics of Major (%) and Trace elements (ppm).

Tabela 1. Estatística descritiva de elementos maiores (%) e elementos traco (ppm).

Elements	n	mean	sd	median	min	max	skew	kurtosis
Major elements (%)								
SiO ₂	156	30.2 6	20.83	29.95	1.36	73.93	0.28	-1.37
Al ₂ O ₃	64	7.93	8.98	4.72	0.05	40.82	1.76	2.36
MgO	63	1.24	0.87	1.34	0.00	3.49	0.43	-0.65
CaO	138	0.42	0.38	0.27	0.01	2.39	1.75	4.43
K ₂ O	129	0.38	0.27	0.34	0.01	1.59	1.36	3.00
Fe ₂ O ₃	156	2.41	1.06	2.35	0.65	8.88	1.54	7.41
MnO	155	0.04	0.04	0.03	0.00	0.18	1.42	1.69
TiO ₂	156	0.45	0.19	0.40	0.09	0.91	0.45	-0.75
P ₂ O ₅	128	0.05	0.04	0.03	0.00	0.18	1.08	0.08
Trace elements (ppm)								
Sr	156	192.95	129.01	154.28	48.53	923.45	2.57	7.74
Rb	156	47.66	18.44	45.72	7.77	101.83	0.38	-0.05
Zr	156	247.89	21.35	248.13	185.58	307.65	-0.22	1.07
V	145	70.13	35.38	67.63	0.50	142.18	0.21	-0.72
Cr	156	79.74	29.67	78.27	28.29	186.82	0.41	0.09
Ni	155	41.57	23.02	40.83	2.42	100.40	0.17	-0.74
Sn	129	54.12	23.63	58.25	1.92	109.55	-0.26	-0.32
Cu	144	39.54	28.88	34.55	0.90	134.31	1.11	0.94
Zn	153	295.02	605.31	168.19	2.59	4971.15	5.07	29.44
Pb	156	93.21	185.95	49.71	26.38	1753.53	6.71	50.44
As	150	22.44	83.24	5.93	0.13	776.11	7.30	57.17
Mo	20	2.97	2.57	1.90	0.09	10.57	1.28	1.32
Ga	3	20.22	19.81	21.03	0.01	39.60	-0.04	-2.33
Nb	153	55.05	22.30	50.65	10.48	131.14	1.30	1.87
Y	156	17.46	9.35	15.34	1.38	53.88	1.26	1.35

the K₂O interpolation shows a unique spatial distribution with higher values in the region on the vicinity of the peralkaline rocks (Fig. 3).

The MnO, V and Zn interpolated maps also show a well-defined contrast between the area located at NW and SE blocks of the Batigelas Fault. The NE-SW Batigelas Fault seems to outline a break in the geochemical pattern following the regional trend, which is visible in the SE block of fault and cryptic in the NW one.

Major elements do not show very strong correlation in any of the cases, nevertheless, Fe₂O₃ shows strong positive correlations with MnO ($r = 0.8$) and TiO₂ ($r = 0.8$), whereas MnO and TiO₂ only display a moderate positive correlation ($r = 0.5$). For the trace elements, Zn shows strong positive correlation with As ($r = 0.8$) and Pb ($r = 0.8$) and both show perfect positive correlation between them ($r = 0.99$); the pairs Sr-Y show perfect positive correlation ($r = 0.95$) and Cu-Nb display strong positive correlation ($r = 0.7$).

4.2. Clustering techniques

Recent works (Fatehi and Asadi, 2017, Zhou *et al.*, 2018, Ghezelbash *et al.*, 2020) use unsupervised machine learning techniques as an aid to refine and detect geochemical anomalies, with special emphasis in clustering methods. Among the

clustering methods applied, hierarchical clustering (hclust) and k-means clustering (k-means) are recognized to provide the most reliable results (*e.g.* Zhou *et al.*, 2018, Ghezelbash *et al.*, 2020).

In the present study, both methods were tested to identify the main geochemical features of the soils in the Batigelas anomaly area and to evaluate their potential applied to *p*XRF data in geochemical exploration.

Before applying the clustering algorithms, a pre-processing data stage must be carried out to assure the trustworthiness of the results.

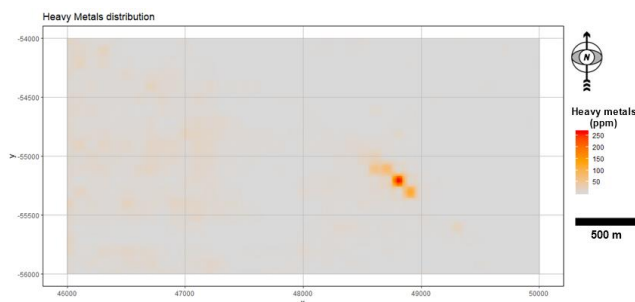


Figure 2. Interpolated geochemical map for the Heavy Metals, based on SFM data.

Figura 2. Mapa de interpolação geoquímica para elementos pesados, baseado em dados do SFM.

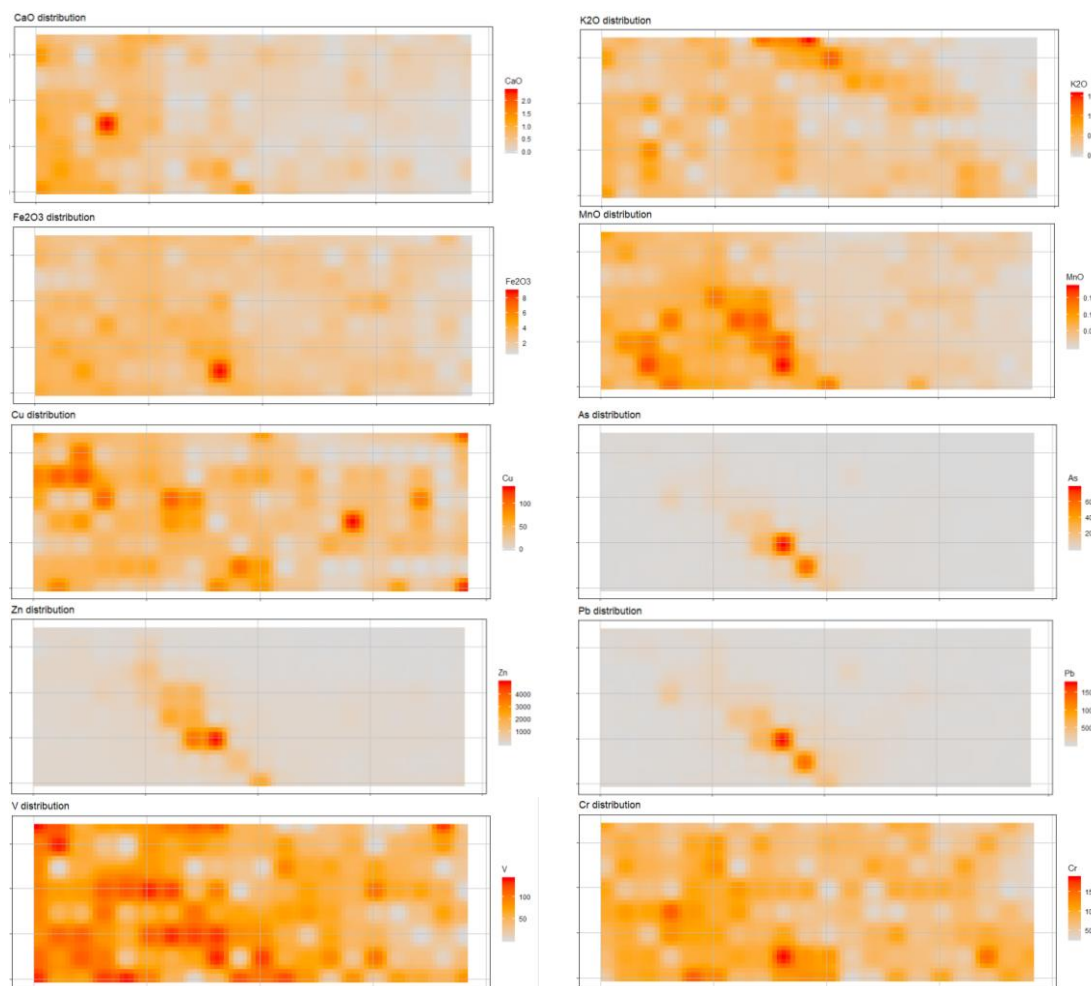


Figure 3. Interpolated maps for selected major elements (CaO, MnO, TiO₂) and for selected trace elements (V, Zn, As). Whereas the major elements and some trace elements (V in the figure but also Cr and Ni) display a gradient that outlines the difference between the main rock formations, some trace elements (*e.g.* Zn and As) are only higher in the vicinity of the mineralized zone. Oxides in %, elements in ppm.

Figure 3. Mapas de interpolação para elementos maiores (CaO, MnO, TiO₂) e elementos traço (V, Zn, As) selecionados. Enquanto que os elementos maiores e traço (V na figura mas também Cr e Ni) traduzam um graiente que põe em evidência as diferenças entre as principais litologias, os elementos traço (*e.g.* Zn e As) apresentam valores mais elevados aóenas nas proximidades da zona mineralizada. Oxidos em % e elementos em ppp.

This stage involves replacing not detected values by the detection limit for each element and the rescaling of the variables, maintaining the distribution but centring all the values to a mean of 0 and a standard deviation of 1, as the elements with different units and interval of representation magnitudes tend to bias the grouping of the variables (Steinley, 2004, Mohamad and Usman, 2013, Kassambara, 2017).

In the unsupervised learning techniques, the number of clusters (*k*) that group the data must be predefined. This work applies the function proposed by Malika *et al.* (2014) for determining the optimal number of clusters; the results suggest two clusters for major elements and, for trace elements, two clusters with hclust and three clusters using k-means. Nevertheless, the two methods were tested with different numbers of clusters (*k*=2, 3, 4) to identify the nature of the chemical elements grouping (Tab. 2, Fig. 4).

For the major elements, hclust and k-means methods grouped the data in the same assemblages (Tab. 2A). For the trace elements the groups defined by both clustering methods are different in some extent (Tab. 2B). In the trials with *k*=2 and *k*=3, depending on the method used, Sn and Cr fall in distinct groups.

For the calculations with *k*=4, Rb, V and Ni also fall in distinct groups; however, *k*=4 clusters revealed to be difficult to interpret, as several elements (Rb, Ni, Cr, V, Sn) are clustered in distinct groups depending on the method used (Tab. 2B).

The only congruent group on what concerns the known geology, regardless of the method used, is the G4 (comprising As, Pb and Zn) which seems to be related with the mineralized zone.

The spatial distribution of the clusters is plotted over the cluster of each observation in the SFM anomaly map (Fig. 4). Maps for *k*=2, *k*=3 and *k*=4 clusters, were created using both hclust and k-means methods, to evaluate their geochemical and geological significance. The major elements *k*=3 and *k*=4 clusters and trace elements *k*=4 cluster were not taken into consideration, because they do not present geological significance. The figure 4 presents the maps of both methods applied to the major elements (*k*=2) and for trace elements (*k*=2 and *k*=3).

Major elements have a similar spatial distribution of the clusters using both methods but are not exactly coincident. Both clustering patterns separate the previously stated areas:

Table 2. List of chemical elements present in each cluster (G1, G2, G3, G4) for major (A) and trace (B) elements and for different number of clusters (k).

Tabela 2. Lista de elementos químicos presentes em cada “cluster” (G1, G2, G3, G4) para elementos maiores (A) e traço (B), bem como para diferentes números de “clusters” (k).

A) Major elements			
	k=2	k=3	k=4
G1	SiO ₂ , K ₂ O, P ₂ O ₅	SiO ₂ , K ₂ O	SiO ₂
G2	CaO, Fe ₂ O ₃ , MnO, TiO ₂	CaO, Fe ₂ O ₃ , MnO, TiO ₂	CaO, Fe ₂ O ₃ , MnO, TiO ₂
G3		P ₂ O ₅	K ₂ O
G4			P ₂ O ₅

B) Trace elements			
	k=2	k=3	k=4
G1	hclust	(Sr, Y, Rb, V, Ni, Zr), Sn, Cr	(Sr, Y, Rb, V, Ni, Zr), Sn, Cr
	k-means	(Sr, Y, Rb, V, Ni, Zr)	(Sr, Y)
G2	hclust	(Zn, Pb, As, Cu, Nb)	(Cu, Nb)
	k-means	(Zn, Pb, As, Cu, Nb), Sn, Cr	(Cu, Nb), Sn, Cr
G3	hclust		(Zn, Pb, As)
	k-means		(Zn, Pb, As)
G4	hclust		(Zn, Pb, As)
	k-means		(Zn, Pb, As)

(G1) comprising SiO₂, K₂O and P₂O₅ (Tab. 2A), is dominant in the northeast area, with conglomerates and peralkaline rocks and

(G2) constituted by CaO, Fe₂O₃, MnO and TiO₂ (Tab. 2A) is dominant in southwest area, representing the calc-silicate and metavolcanic rocks (Fig. 1).

The trace elements have significant differences that are dependent on the clustering method applied:

- For k=2, k-means separates the lithological units (G1 [Sr, Y, Rb, V, Ni, Zr]; Tab. 2B) from the mineralized zone (G2 [Zn, Pb, As, Cu, Nb]; Tab. 2B). The hclust method does not discriminate the mineralized zone, only showing two distinct geochemical units;

- For k=3, k-means clustering map shows three geochemical units, namely the two previously mentioned lithological areas (G1 [Sr, Y, Rb, V, Ni, Zr] and G2 [Cu, Nb, Sn, Cr]; Tab. 2B) and the mineralized zone (G3 [Zn, Pb, As]; Tab. 2B). The hclust method also discriminates the same three geochemical units, although with high dispersion of G1 and G2 geochemical units, with a poorly defined cluster representing the geochemical anomaly (G3).

For this study case, all these observations suggest that k-means clustering method, for k=2 and k=3, provides a better correspondence with the known geochemical anomaly, whereas using the hclust method the anomaly is not so obvious (Fig. 4).

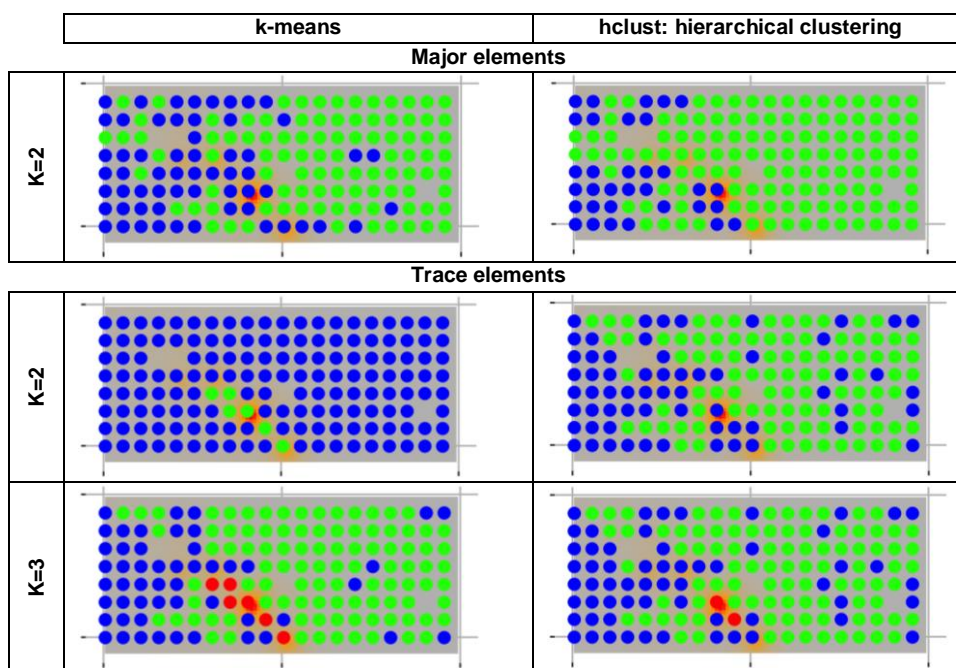


Figure 4. Cluster analyses for major and trace elements. Background image is based on the heavy metals map of figure 2. Each dot color (blue, green and red) represents a cluster.

Figura 4. Análise cluster dos elementos maiores e traço. A imagem de background baseia-se no mapa de elementos pesados da figura 2. A cor de cada ponto (azul, verde e vermelho) representa um cluster.

5. Discussion and final remarks

The feasibility of the pXRF in geochemical exploration was proved to be an excellent tool (as also reported by Lemiere, 2018), detecting and quantifying a significant number of elements for high resolution geochemical mapping, allowing to discriminate distinct geochemical units (concordant with regional NW-SE trend) with distinct clustering methods, thus providing fast plausible *in situ* results.

The interpolated maps (of major and trace elements) are a trustworthy tool for identifying the main geochemical trends and, in some specific cases, can even be correlated with individual lithological units and structures, for example in the case of the peralkaline rocks or the Batigelas Fault. The presumably mineralized zone identified by SFM studies was detected with interpolation methods, demonstrating that this combination of techniques might be used in mineral exploration campaigns, providing fast and detailed results with cost-effectiveness.

The application of the clustering techniques used for both major and trace elements is only applicable with advantage in some cases. In the study case, major elements generated the same groups and similar patterns independently of the clustering method used.

The k-means clusters are well superimposed with the SFM anomaly (*i.e.* mineralized zone), regarding a significant number of soil analyses with high Pb, Zn and As content. The hclust method was also able to identify the geochemical anomaly when defining three clusters but restricts the anomalous zone to a narrow area.

The trace element grouping with both methods clustered Pb, Zn and As, all susceptible to be incorporated in the same mineral lattice. The anomalous values of Zn and Pb superimposed with the geochemical anomaly of SFM and the high correlation with pathfinder elements as As, Fe₂O₃ and MnO (*e.g.* Leach *et al.*, 1986; D'Ercole *et al.*, 2000) suggests the presence of a possible Zn-Pb deposit. Additionally, the structural and stratigraphic settings of the detected anomaly (NW-SE direction, parallel to regional trend), which are located within a geological contact between two distinct lithological units, are in accordance with a strata-hosted Zn and Pb deposit, similar to other deposits identified in the OMZ carbonate formations (Mateus *et al.*, 2013; Matos and Filipe, 2013). The geochemical clustering here presented and the published data regarding the mineralization derived with the mafic-ultramafic plutonics (*e.g.* Pinto *et al.*, 2006; Mateus *et al.*, 2013 and references therein) seems to demonstrate that Batigelas anomaly is not related with the Alter do Chão – Cabeço de Vide complex.

The combination of traditional single element geochemical mapping with machine learning clustering techniques provides a better understanding of the geochemical features of group elements, thus being useful when detecting multi-elemental assemblages and/or pathfinders in ore deposits exploration campaigns. Nevertheless, future petrological, structural and stratigraphic studies must sustain all these assumptions.

Acknowledgments

This work is a contribution to the project ZOM3D: ALT20-03-0145-FEDER-000028, funded by Alentejo 2020 through the FEDER/FSE/FEEI. The authors also acknowledge the funding provided to Institute of Earth Sciences through the COMPETE 2020 project (UIDB/GEO/04683/2020) under the reference POCI-01-0145-FEDER-007690. The authors acknowledge the two revisors, T. Albuquerque and M. Anjos Ribeiro, for their contributions and insights.

Referências

- Afonso, P. (in prep.). *Geofísica e Química Mineral na região de Batigelas, Zona Ossa-Morena. Um caso de estudo de ocorrências de metais básicos no Setor de Alter do Chão – Elvas*. Master Thesis. University of Évora.
- Araújo, A., Piçarra de Almeida, J., Borrego, J., Pedro, J., Oliveira, T., 2013. As regiões central e sul da Zona de Ossa-Morena. In: Dias, R., Araújo, A., Terrinha, P., Kullberg, J. C. (Eds.), *Geologia de Portugal*, Escolar Editora, 1: 509-549.
- Bourke, A., Ross, P. S., 2016. Portable X-ray fluorescence measurements on exploration drill-cores: comparing performance on unprepared cores and powders for whole-rock analysis. *Geochem-Explor. Env. A.*, **16**(2): 147-157. DOI: 10.1144/geochem2014-326.
- Carrilho Lopes, J. M., Sant'Ovaia, H. Gomes, C., 2013. Update of Geochemical and Geochronological data of the Santa Eulália Plutonic Complex (Alentejo, Portugal). *Colóquio Anisotropia da Susceptibilidade Magnética, Tectónica e (Paleo)magnetismo dos materiais*, Universidade de Coimbra, 5.
- Carrilho Lopes, J., 1989. *Geoquímica de Granitóides Hercínicos na Zona de Ossa-Morena: O Maciço de St.ª Eulália*. Provas de aptidão pedagógica e capacidade Científica (Unpublished), 138.
- Carrilho Lopes, J.; Ferreira, M., Munhá, J. 1993. Geochronological relationships between the Alter do Chão-Cabeço de Vide basic/ultrabasic massif and peralkalini rocks in NE-Alentejo. *Terra Nova*, **5**: 15.
- D'Ercole, C., Groves, D. I., Knox-Robinson, C. M., 2000. Using fuzzy logic in a Geographic Information System environment to enhance conceptually based prospectivity analysis of Mississippi Valley-type mineralisation. *Australian J. Earth Sci.*, **47**(5): 913-927. DOI: j.1440-0952.2000.00821.x.
- De Oliveira, D. P., Reed, R. M., Milliken, K. L., Robb, L. J., Inverno, C. M. C., Orey, F. D., 2003. Série Negra black quartzites-Tomar Cordoba Shear Zone, E Portugal: mineralogy and cathodoluminescence studies. *Cad. Lab. Xeol. Laxe*, **28**: 193-211.
- Díez Fernández, R., Pereira, M. F., Foster, D. A., 2015. Peralkaline and alkaline magmatism of the Ossa-Morena zone (SW Iberia): Age, source, and implications for the Paleozoic evolution of Gondwanan lithosphere. *Lithosphere*, **7**(1): 73-90. DOI: 10.1130/L379.1.
- Fatehi, M., Asadi, H. H., 2017. Application of semi-supervised fuzzy means method in clustering multivariate geochemical data, a case study from the Dalli Cu-Au porphyry deposit in central Iran. *Ore Geol. Rev.*, **81**: 245–255. DOI: 10.1016/j.oregeorev.2016.10.002.
- Ghezalbash, R., Maghsoudi, A., Carranza, E., 2020. Optimization of geochemical anomaly detection using a novel genetic K-means clustering (GKMC) algorithm. *Comp. Geosci.*, **134**: 104335. DOI: 10.1016/j.cageo.2019.104335.
- Gonçalves, F., 1972. *Folha 32-B Portalegre da Carta Geológica de Portugal, na escala de 1:50 000*. Serviços Geológicos de Portugal, Lisboa.
- Hall, G., Page, L., Bonham-Carter, G., 2013. *Quality Control Assessment of Portable XRF Analysers: Development of Standard Operating Procedures, Performance on Variable Media and Recommended Uses. Phase II*. Canadian Mining Industry Research Organization (Camiro) Exploration Division, Project 10E01 Phase I Report.
- Hou, X., He, Y., Jones, B. T., 2004. Recent advances in portable X-ray fluorescence spectrometry. *App. Spectr. Rev.*, **39**(1): 1-25. DOI: 10.1081/ASR-120028867.
- Isaaks, E. H., Srivastava, R. M., 1989. *An Introduction to applied geostatistics*. New York: Oxford University Press.
- Kassambara A., 2017. *A practical guide to cluster analysis in R. Unsupervised machine learning*. STDHA editions, 187.
- Lancelot, J. R., Allegret A., 1982. Radiochronologie U-Pb del'orthogneiss alcalin de Pedroso (Alto Alentejo, Portugal) et evolution ante hercynienne de l'Europe occidentale. *Neues Jahrb. Mineral. Monatsh.*, 385-394.
- Leach, D. L., Viets, J. B., Foley-Ayuso, N., Klein, D. P., 1995. Mississippi Valley-type Pb-Zn deposits. Preliminary compilation of descriptive geoenvironmental mineral deposit models. *US Geological Survey Open-File Report*, 234-243.
- Lemiere, B., 2018. A Review of pXRF (Field Portable X-ray Fluorescence) Applications for Applied Geochemistry. *J. Geochem. Expl.*, **188**: 350-363. DOI: 10.1016/j.gexplo.2018.02.006.

- Malika, C., Ghazzali, N., Boiteau, V., Niknafs, A., 2014. NbClust: An R Package for Determining the Relevant Number of Clusters in a Data Set. *J. Stat. Softw.*, **61**: 1-36.
- Mateus, A., Munhá, J., Inverno, C., Matos, J. X., Martins, L., Oliveira, D., Jesus, A., Salgueiro, R., 2013. Mineralizações no sector português da Zona de Ossa-Morena. In: Dias, R., Araújo, A., Terrinha, P., Kullberg, J. C. (Eds.), *Geologia de Portugal*, Escolar Editora, **1**: 577-619.
- Matos, J. X., Filipe, A. (coord.), 2013. *Carta de Ocorrências Mineiras do Alentejo e Algarve, Escala 1:400 000*. Laboratório Nacional de Energia e Geologia, 1st Edition. ISBN: 978-989-675-029-9.
- Mohamad, I. B., Usman D., 2013. Standardization and Its Effects on K-Means Clustering Algorithm. *Res. J. App. Sci., Eng.Tech.*, **6**(17): 3299-3303. DOI:10.19026/rjaset.6.3638.
- Moreira, N., Dias, R., Pedro, J. C., Araújo, A., 2014a., Interferência de fases de deformação Varisca na estrutura de Torre de Cabedal; sector de Alter-do-Chão – Elvas na Zona de Ossa-Morena. *Comun. Geol.*, **101**(1): 279-282.
- Moreira, N., Araújo, A., Pedro, J., Dias, R., 2014b. Evolução Geodinâmica na Zona de Ossa-Morena no contexto do SW Ibérico durante o Ciclo Varisco. *Comun. Geol.*, **101**(1): 275-278.
- Oliveira, J. T., Oliveira, V., Piçarra, J. M., 1991. Traços gerais da evolução tectono-estratigráfica da Zona de Ossa-Morena. *Cad. Lab. Xeol. Laxe*, **16**: 221-250.
- Pereira, M. F., Chichorro, M., Linnemann, U., Eguiluz, L., Silva, J. B., 2006. Inherited arc signature in Ediacaran and Early Cambrian basins of the Ossa-Morena zone (Iberian Massif, Portugal): paleogeographic link with European and North African Cadomian correlatives. *Precamb. Res.*, **144**(3-4): 297-315. DOI: 10.1016/j.precamres.2005.11.011.
- Pereira, M. F., Chichorro, M., Solá, A. R., Silva, J. B., Sánchez-García, T., Bellido, F., 2011. Tracing the Cadomian magmatism with detrital/inherited zircon ages by in-situ U-Pb SHRIMP geochronology (Ossa-Morena zone, SW Iberian Massif). *Lithos*, **123**: 204-217. DOI: 10.1016/j.lithos.2010.11.008.
- Pereira, M. F., Gama, C., Rodríguez, C., 2017. Coeval interaction between magmas of contrasting composition (Late Carboniferous-Early Permian Santa Eulália-Monforte massif, Ossa-Morena Zone): field relationships and geochronological constraints. *Geologica Acta*, **15**(4): 409-428. DOI: 10.1344/GeologicaActa2017.15.4.10.
- Pinto, Z. A., Pañeda, A., Castelo Branco, J. M., Leal Gomes, C., Dias, P. A. 2006. Cartografia Geológica do Complexo básico – ultrabásico de Castelo de Vide – Ensaio sobre a geometria e potencial metalogenético. *VII Congresso Nacional de Geologia*, 1051-1054.
- R Core Team, 2014. *R: A language and environment for statistical computing*. R Foundation for Statistical Computing, Vienna, Austria.
- Sant’Ovaia, H., Nogueira, P., Carrilho Lopes, J., Gomes, C., Ribeiro, M. A., Martins, H. C. B., Dória, A., Cruz, C., Lopes, L., Sardinha, R., Rocha, A., Noronha, F., 2015. Building up of a nested granite intrusion: magnetic fabric, gravity modelling and fluid inclusion planes studies in Santa Eulália Plutonic Complex (Ossa Morena Zone, Portugal). *Geol. Mag.*, **152** (4): 648-667. DOI: 10.1017/S0016756814000569.
- Serrano Pinto, M., 1984. Granitóides caledónicos e hercínicos na zona de Ossa-Morena (Portugal). Nota sobre aspectos geocronológicos. *Memórias e notícias. Publicações do Museu e Laboratório mineralógico e geológico da Universidade de Coimbra*, **97**: 81-94.
- Steinley, D., 2004. Standardizing Variables in K-means Clustering. In: Banks D., McMorris F. R., Arabie P., Gaul W. (Eds.) *Classification, Clustering, and Data Mining Applications. Studies in Classification, Data Analysis, and Knowledge Organisation*. Springer, Berlin, Heidelberg, 53-60.
- Zhou, S., Zhou, K., Wang, J., Yang, G., Wang, S., 2018. Application of cluster analysis to geochemical compositional data for identifying ore-related geochemical anomalies. *Front. Earth Sci.*, **12**: 491. DOI: 10.1007/s11707-017-0682-8